Advances in Environmental Technology 12(3) 2026, 308-327.

Iranian Reasearch Organization for Science and Technology (IROST)

Advances in Environmental Technology

Journal home page: https://aet.irost.ir

Adsorption of hexavalent chromium from aqueous solution using glucose-derived spherical activated carbon: The role of functional groups

Nguyen Duy Dat[a]*, Quang Sang Huynh[a], My Linh Nguyen[a], Hai Nguyen Tran[b]

[a] *Faculty of Chemical and Food Technology, Ho Chi Minh City University of Technology and Engineering, Viet Nam.*

[b] *Institute of Fundamental and Applied Sciences, Duy Tan University, Ho Chi Minh City 70000, Viet Nam.*

ARTICLE INFO

Document Type:
Research Paper

Article history:
Received 23 September 2025
Received in revised form
24 April 2026
Accepted 26 April 2026

Keywords:
Adsorption mechanism
Functional groups
Hexavalent chromium
Hydrothermal synthesis
Spherical activated carbon

ABSTRACT

This research explores the production of spherical activated carbon derived from glucose using the combination of a hydrothermal process followed by chemical impregnation with hydrogen peroxide (H_2O_2), citric acid (CA), and acrylic acid (AA), and pyrolysis. The adsorption performances, kinetics, and thermodynamics of the synthesized materials were compared with those of the material without chemical impregnation using batch experiments. Boehm titration and Fourier-transform infrared spectroscopy (FTIR) confirmed an increase in oxygen-containing functional groups (carboxyl, lactone, and phenol), facilitating adsorption through electrostatic interaction, reduction, and complexation. Adsorption kinetics and isotherm modeling confirmed that the process adhered to the Elovich model and the Redlich-Peterson or Langmuir isotherm, suggesting chemisorption dominance. Among the materials tested, AA-modified activated carbon (AC-AA) exhibited the highest adsorption capacity of 244 mg/g, outperforming previously studied biochar-based adsorbents. Kinetic and thermodynamic assessments demonstrated that Cr(VI) adsorption was spontaneous ($\Delta G<0$), endothermic ($\Delta H>0$), and entropy-favored ($\Delta S>0$). Notably, the study elucidates the concurrent adsorption and reduction of Cr(VI) to Cr(III) at low pH, driven by electron transfer from surface functional groups. Moreover, NaOH was identified as the most effective desorption agent, underscoring the potential for material regeneration and reuse. This research highlights the potential application of glucose-based carbon spheres with functionalized surfaces as a sustainable, cost-effective solution for Cr(VI) removal in industrial wastewater treatment.

*Corresponding author Tel.: +84 903 056285
E-mail: datnd@hcmute.edu.vn
DOI: 10.22104/aet.2026.7860.2207

1. Introduction

A wide range of human activities, such as industrial processes, agricultural practices, and transportation, release heavy metals that can directly contaminate water sources or disperse into the atmosphere, settle as dust, and eventually be carried into waterways, resulting in substantial water pollution [1, 2]. For example, the application of pesticides, particularly phosphorus fertilizers, can result in the discharge of toxic metals, such as arsenic (As), lead (Pb), and mercury (Hg), into water bodies [3]. The presence of heavy metals in aqueous effluents is a significant concern due to their toxicity and carcinogenic effects on aquatic life and human health [4]. Heavy metals have long-lasting characteristics in the environment, resulting in a range of health problems: dissolve in water, build up in plants and animals, and enter the human food chain via polluted water or food [5]. The unregulated release of heavy metals into the environment presents substantial hazards due to their poisonous impact on living creatures [6].

Out of all these metals, chromium stands out as particularly remarkable in two prevalent forms, in which hexavalent chromium (Cr(VI)) is more toxic than trivalent chromium (Cr(II)), causing severe health issues, including cancer, respiratory problems, and skin ulcers [7, 8]. According to the World Health Organization (WHO), hexavalent chromium is categorized as a carcinogen and is considered one of the 50 most dangerous compounds worldwide [9, 10]. It is commonly detected in soil and groundwater in industrial locations as a result of its use in dyes, paints, and tannery wastewater [11]. While the volume of wastewater generated by electroplating and metal plating companies may not be as substantial as that of other sectors, such as paper or textile industries, it does include significant amounts of dangerous substances, notably chromium [12].

The study of heavy metal removal from water via adsorption has been extensively explored worldwide. A previous study investigated the use of agricultural by-products, such as bagasse, banana peels, coconut fiber, sawdust, corn husks, rice husks, straw, and peanut shells, for heavy metal removal in water by employing adsorption on these modified materials with phosphoric acid [13]. Similarly, the previous study prepared biochar from Tectona grandis sawdust, activating it with K_2CO_3 and $ZnCl_2$, which achieved a surprisingly high Cr(VI) maximum adsorption capacity ranging from 103 mg/g to 127 mg/g [14]. A maximum chromium adsorption capacity of 176 mg/g was obtained using KOH-modified activated carbon derived from corn straw [15]. Additionally, activated carbon (AC) prepared from waste tire material demonstrated a high chromium adsorption capability of 55.2 mg/g, while apple peel processed with modified H_3PO_4 showed a maximum chromium adsorption capacity of 36 mg/g [16]. Nevertheless, some studies have enriched functional groups on the surface of activated carbon using HNO_3, resulting in a surface area of 1399 m^2/g and an enhancement of lactone functional groups [17]. With the addition of functional groups, such as –OH, –C=O, –P=O, –P–O–C, and numerous carbon-carbon bonds, the process of impregnating AC with H_3PO_4 also contributes to an increase in surface area to 1290 m^2/g [18]. These studies suggested that modifications to cellulose-based materials can enhance their adsorption capacity.

The hydrothermal carbonization (HTC) approach utilizes an aqueous solution and operates at low temperatures ranging from 160 to 220 °C, which is environmentally friendly, uncomplicated, and economically advantageous [19, 20]. Biomass materials are optimal carbon sources for producing high-capacity capacitor materials by HTC due to their renewability, high reactivity, and low cost. Lignocellulosic biomass, which consists mainly of glucose, may be efficiently carbonized using HTC to generate well-organized carbon spheres that possess a highly porous structure and significant surface area [21]. As an illustration, a previous study documented a specific surface area (S_{BET}) of 1282.8 m^2/g and a micropore volume (V_{micro}) of 0.44 cm^3/g obtained from glucose utilizing KOH activation via the hydrothermal technique [22]. Acid modification, which mostly involves the use of hydrochloric acid, nitric acid, or phosphoric acid, changes the surface area of activated carbon to increase its capacity to absorb contaminants [23-25]. In one example, the adsorption performance was significantly enhanced after chemical activation with H_3PO_4; the mesopore volume and

specific surface areas of orange peel-derived carbon were enhanced from 0.025 cm^3/g and 117 m^2/g to 0.102 cm^3/g and 618 m^2/g, respectively [26].

The main objective of alkaline treatment (with substances like potassium hydroxide, sodium hydroxide, etc.) was to increase the number of functional groups containing oxygen and particular surface areas [27, 28]. As an illustration, industrial alkali lignin was employed to create a hierarchical porous carbon-based adsorbent (L-HPC) for the combined hydrothermal and alkali activation processes to adsorb Cr (VI) [26]. During the KOH treatment, a few three-dimensional linked channels were formed, and numerous active groups, such as those containing N and O, were produced. Hydrothermal carbon nanospheres (CNS) were made from glucose and activated with aqueous NaOH solutions. The outcomes showed that the NaOH solution-impregnated CNS surface was enhanced with –OH and –COO–, significantly changing the morphology, surface area, and pore volume [29]. Overall, the modification or activation of carbon can be a useful method to obtain adsorbents with high surface area and functional groups that are beneficial for the adsorption process.

Therefore, this study aimed to investigate the influence of different chemical agents, including Acrylic Acid (AA), Citric Acid (CA), and H_2O_2, used to activate hydrochar derived from the hydrothermal process of glucose. Additionally, this study assessed the effects of bath operating parameters on the adsorption performance of achieved materials: pH, temperature, contacting time, initial concentration of Cr(VI), and different background water sources. The adsorption mechanisms of the adsorption process were elucidated using kinetic, thermodynamic, and adsorption isotherm models. Furthermore, adsorption mechanisms associated with the removal of Cr(VI) in water solution were discussed in this study.

2. Materials and methods

2.1. Reagents

In this study, glucose ($C_6H_{12}O_6$), potassium dichromate ($K_2Cr_2O_7$), sulfuric acid (H_2SO_4), sodium hydroxide (NaOH), hydrochloric acid (HCl), hydrogen peroxide (H_2O_2), citric acid ($C_6H_8O_7$), acrylic acid ($C_3H_4O_2$), and 1,5 Diphenylcarbazide were obtained from Alpha Chemical Reagent Co., Ltd. (Tianjin, China) and qualified as analytical grade. All working solutions used during all experiments were prepared by diluting chemicals in deionized water.

2.2. Preparation of materials

The materials were synthesized from glucose through hydrothermal, impregnation, and pyrolysis steps as shown in Figure 1. The glucose hydrochar (GH) was produced by the hydrothermal method using 32.4g glucose with 120 mL deionized (DI) water in a Teflon-lined stainless steel autoclave at 190 °C for 24 h [30]. The GH was washed with alcohol (95%) and distilled water until the pH value was equal to that of the DI water. Subsequently, 3.0g HG was impregnated with 50 mL of chemical agents, including H_2O_2, acrylic acid (AA), and citric acid (CA) with a concentration of 0.3 M for 24 h. After the materials were washed and dried, they were pyrolyzed at 900 °C for 2 h under atmospheric conditions at a rate of 45 ℃/min and 0.5 L N_2/min. The materials were washed with DI water until the pH value remained constant, and then dried and sieved to a size of 0.088 mm. Four materials obtained, as described in Figure 1, will be compared in this study to clarify the influence of chemical agents on Cr(VI) adsorption in aqueous solution.

2.3. FT-IR analysis, pHpzc analysis, and the acidic and basic groups

Their surface morphology was displayed using scanning electron microscope (SEM) images (JSM-6510 LV; Japan). Fourier-transform infrared spectroscopy (FTIR; FT/IR-4600; Japan) determined the main functional groups on their surface.

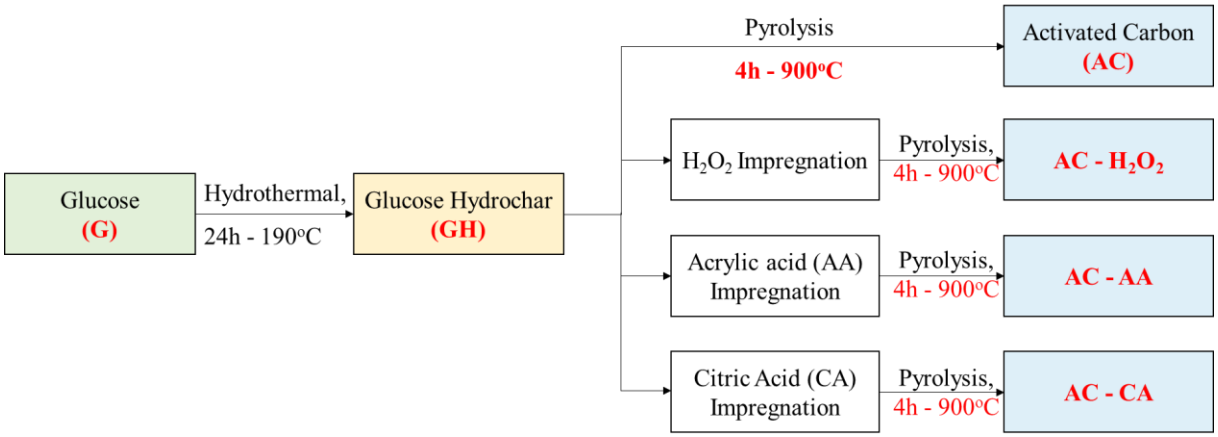

Fig. 1. Synthetic process of materials.

The drift method was used to estimate the pH value of the material's point zero charges (pH_{PZC}) [23]. The acidic and basic groups on the adsorbent surfaces were determined by Boehm titration by the technique described in the previous study, which can quantify carboxylic, phenolic, and lactonic functional groups of pristine and laden materials [30].

2.4. Adsorption - Desorption experiments

The adsorption experiments were conducted in a batch reactor with a solid/liquid ratio of 0.5 g/L in a thermostatic shaker. The appropriate concentration of Cr(VI) solution was obtained by dissolving $K_2Cr_2O_7$ in DI water.

The diphenylcarbazide method was used to measure the concentration of Cr (VI) before and after the adsorption process [31]. Diphenylcarbazide forms a red-violet complex with Cr(VI), and the intensity of this complex was detected at 542 nm with a UV–vis spectrophotometer (Hitachi U-2910, Hitachi Corp., Japan). Furthermore, the total concentration of Cr before and after adsorption was analyzed by the atomic absorption spectroscopy technique (AAS - Hitachi ZA3300, Hitachi Corp., Japan). Cr(VI) concentrations were determined, and the adsorption capacity was calculated by Eq. (1) at defined time intervals until reaching adsorption equilibrium after samples were taken and filtered through a 0.45-µm Whatman membrane filter.

$$q_e = \frac{(C_0 - C_e) \times V}{m} \quad (1)$$

Where C_e (mg/L) is the Cr(VI) concentration at equilibrium, C_0 (mg/L) is the initial concentration of Cr(VI), q_e (mg/g) is the adsorption capacity at equilibrium, V (L) is the volume of Cr(VI) solution, and m (g) is the mass of the adsorbent.

To investigate the influence of desorption taken by different extraction solutions, the laden adsorbent was shaken with 200 mL of various desorbing agents, including hot water at 60°C, NaOH (0.05 M), and HCl (0.05 M). The percentage of adsorbates desorbed (R_{Des}) from the laden adsorbent was calculated via Eq.(2).

$$R_{Des} = \frac{q_{e(2)}}{q_{e(1)}} \times 100\% \quad (2)$$

where $q_{e(1)}$ (mg/g) and $q_{e(2)}$ (mg/g) are the adsorption capacities of materials at the first and second cycles of adsorption and desorption, respectively.

2.5. Isotherm models, adsorption kinetics, and thermodynamics

Three models were studied to investigate the equilibrium parameters, including the Langmuir, Freundlich, and Redlich-Peterson models [32]. The Redlich-Peterson isotherm was proposed in response to the limitations of the Freundlich and Langmuir isotherms. This model combines aspects of the Freundlich and Langmuir models and might be used to demonstrate adsorption equilibrium across a wide range of adsorbate concentrations [33]. Langmuir, Freundlich, and Redlich-Peterson models were defined as Eq. (3), (4), and (5), respectively.

$$q_e = \frac{q_{max} K_L C_e}{1 + K_L C_e} \quad (3)$$

where q_{max} (mg/g) is the maximum adsorption capacity, and K_L is the Langmuir constant.

$$q_e = K_F C_e^{1/n} \quad (4)$$

where n is the adsorption intensity, and K_F is the Freundlich constant.

$$q_e = \frac{K_{RP} C_e}{1 + a_{RP} C_e^g} \quad (5)$$

where K_{RP} and a_{RP} $(mg/L)^{-g}$ are the Redlich–Peterson constants, and g is an exponent which must lie between 0 and 1.

Kinetic parameters were studied using the pseudo-first-order (PFO) model, the pseudo-second-order (PSO) model, and the Elovich model. The PFO and PSO models were defined as Eq. (6) and (7) [32], respectively. While the Elovich [33] model was defined as Eq. (8).

$$q_t = q_e (1 - e^{-k_1 t}) \quad (6)$$

$$q_t = \frac{q_e^2 k_2 t}{1 + k_2 q_e} \quad (7)$$

where q_t (mg/g) is the adsorption capacity at contacting time t; k_1 and k_2 are the pseudo-first order and pseudo-second order kinetic rate constants, respectively.

$$q_t = \frac{1}{\beta}\ln(t) + \frac{1}{\beta}\ln(\alpha\beta) \quad (8)$$

where α (mg/g.min) is the initial rate constant, and β (mg/g) is the desorption constant.

To investigate the effect of temperature on the adsorption process, enthalpy changes (ΔH°, kJ/mol), entropy (ΔS°, kJ/mol), and Gibbs free energy (ΔG°, kJ/mol) were studied using Eqs. (9) - (12). The thermodynamic parameters can be estimated using the following equations based on thermodynamic standards [34].

$$\Delta G° = -RT\ln K_c \quad (9)$$

The following describes the relationship of ΔG° to ΔH° and ΔS°:

$$\Delta G° = \Delta H° - T\Delta S° \quad (10)$$

$$\ln K_c = \frac{-\Delta H^o}{R} \times \frac{1}{T} + \frac{\Delta S^o}{R} \quad (11)$$

$$K_c = \frac{MW \times 1000 \times K_L}{\gamma} \quad (12)$$

where K_c is the equilibrium constant, K_L is Langmuir constant (L/mg), MW is molecular mass of the pollutant (g/mol), R is the universal gas constant (8.3144 J/mol K), and T is absolute temperature in Kelvin (K).

All experiments were conducted in triplicate. The reported results represent the average values of the three independent measurements. In Figures 3, 6, 7, and 8, the error bars indicate three standard deviations (±3 SD).

3. Results and discussion

3.1. SEM, FTIR, and pH_{pzc} analysis

The SEM image (Figure 2a) reveals interconnected spheres with smooth outer surfaces, regular spherical shapes, consistent diameters, and high purity.

The FTIR spectrum of spherical biochar and spherical activated carbon materials demonstrated the typical characteristics of the adsorbent shown in Figure 2b. The (–OH) stretching vibrations in the hydroxyl groups of hemicellulose, cellulose, and lignin are responsible for the bands at 3700–3000 cm^{-1} [35].

The bands at 1800-1650 cm^{-1} are evidence of carboxylic and lactonic groups (C=O) [36]. Likely, the C=C double bonds in aromatic rings are responsible for the bands that ring the region between 1650 and 1480 cm^{-1}. The bands in the 970–730 cm^{-1} range, which are associated with the aromatic C–H out-of-plane bending mode, can also be used to identify the presence of aromatic benzene rings [37, 38].

Lastly, stretched C=O groups can be seen in bands between 1290 and 970 cm^{-1} [39]. As shown in Figure 2b, the intensity of the –OH, C–H, C=O, and C–O peaks in the AC-AA and AC-CA was greater than that of AC, indicating that impregnation in acrylic acid and citric acid can increase these functional groups. The previous research indicated that these groups are features of the carboxylic functional group, which is effective in removing Cr(VI) [40].

The AC material exhibits a remarkable BET-specific surface area of 770 m^2/g and a substantial pore volume of 0.384 cm^3/g, which are highly conducive to its exceptional adsorption affinity for a wide range of contaminants.

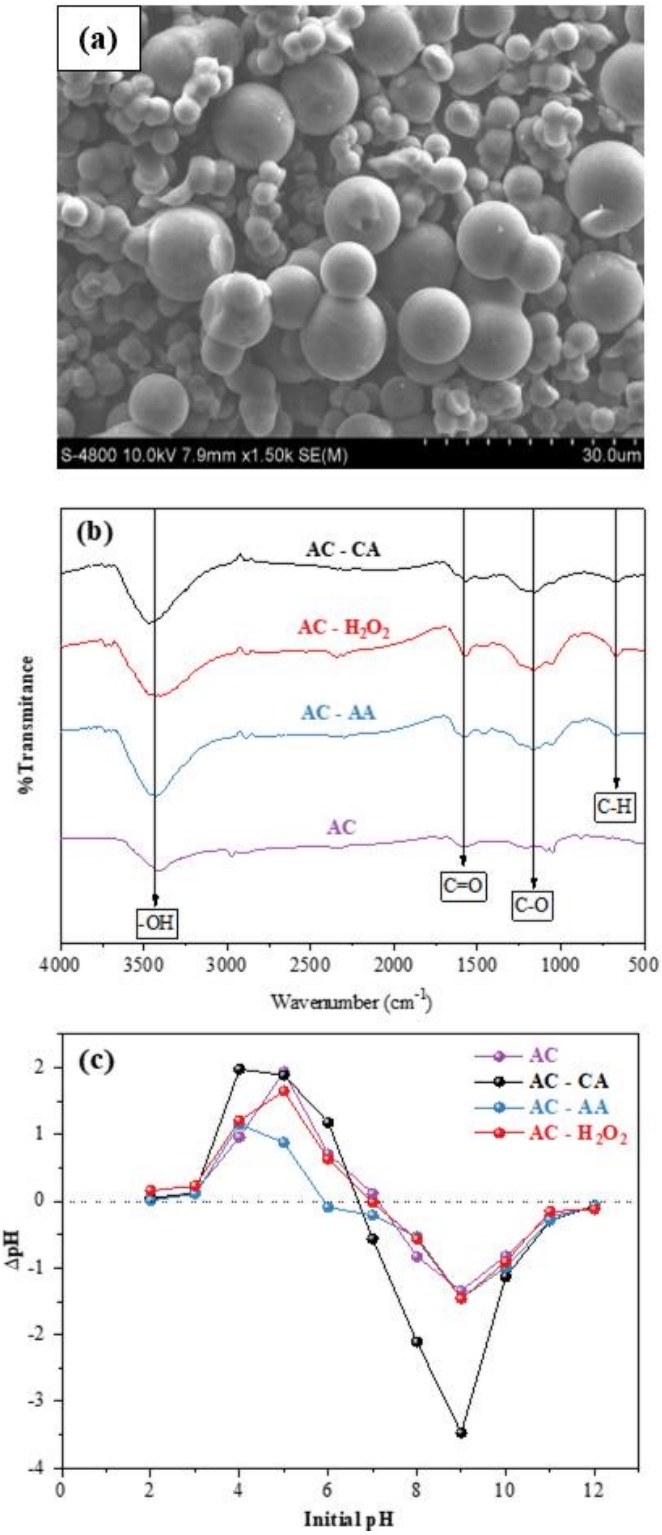

Fig. 2. SEM image of (a) AC, (b) FTIR analysis, and (c) pH_{PZC} analysis of materials.

The point of zero charges (PZC) was a defining characteristic of the electrical state of the adsorbent surfaces in solutions. The value of pH_{PZC} refers to the pH level at which an adsorbent's net (internal and external) surface charge is zero. Plot and pH_{PZC} values of adsorbent samples obtained using the pH drift method are shown in Figure 2c. The pH_{PZC} of the materials followed the order of AC (7.1) > AC-H_2O_2 (6.98) > AC-AA (5.89) > AC-CA (5.58), indicating that chemical agents had a significant impact on the pH_{PZC} values of the absorbent.

3.2. The acidic and basic groups

The results of qualifying three common functional groups in synthesized materials before and after adsorption are presented in Table 1. The results showed that total functional groups measured before adsorption of AC-AA were the highest with 4.02 (mmol/g), followed by AC-CA (3.61 mmol/g), and AC-H_2O_2 (2.47 mmol/g); the lowest was AC with (1.54 mmol/g). These findings indicate that chemical agents can effectively increase functional groups in materials regardless of pyrolysis at 900 ℃ after impregnation, which is in agreement with FTIR results (Figure 2b). The results also indicated that impregnating the materials with AA, CA, and H_2O_2 can at least double the carboxylic group content while reducing the phenolic group content. On the other hand, impregnating GH in AA, CA, and H_2O_2 can increase lactonic groups about 13, 15, and 4 times, respectively, compared to AC. Among the three functional groups, the carboxylic functional group had the highest content on the surface of materials, which can facilitate the adsorption of Cr(VI) through the complexation mechanism [41].

The lactonic group was indicated as a key functional group in removing Cr(VI) in water [42]. Table 1 also reveals that impregnation of GH in AA and CA can effectively enhance carboxylic and lactonic groups on the surface of ACs. The reduction of these functional groups after treatment might imply that these groups play a vital role in the adsorption of Cr(VI) in water.

Table 1. Quantification of functional groups in synthesized materials before and after adsorption.

	Before adsorption (mmol/g)				After adsorption (mmol/g)			
Adsorbent	**Carboxylic**	**Phenolic**	**Lactonic**	**Total**	**Carboxylic**	**Phenolic**	**Lactonic**	**Total**
AC	1.05	0.41	0.08	1.54	0.22	0.14	0	0.36
AC-CA	2.09	0.34	1.18	3.61	0.67	0.16	0.13	0.96
AC-AA	2.89	0.11	1.02	4.02	0.94	0.05	0.17	1.16
AC-H_2O_2	2.12	0.04	0.31	2.47	0.49	0	0.18	0.67

3.3. Effects of pH and contacting time

The pH of the solution is one of the most important parameters influencing heavy metal ion adsorption from aqueous solutions, as it directly affects the charge density on the surface of the adsorbent and the charge of the metallic species present [23]. The effect of solution pH on Cr(VI) adsorption by adsorbent materials is shown in Figure 3a. The removal of Cr(VI) from an aqueous solution is highly dependent on pH values, with maximal adsorption occurring when the pH is 2.0. The speciation of Cr(VI) in aqueous solution with varying pH has shown different anion forms, including H_2CrO_4, $HCrO_4^-$, CrO_4^{2-}, or $Cr_2O_7^{2-}$ [43]. In the pH range of 2.0 to 6.0, the ions $HCrO_4^-$ and $Cr_2O_7^{2-}$ are mostly in equilibrium; $HCrO_4^-$ dominates in solution at pH 2, which will transfer to a chromate ion (CrO_4^{2-}) as the pH increases [44]. During adsorption, a chromate ion (CrO_4^{2-}) requires two active sites, while an $HCrO_4^-$ ion requires only one active site. As a result, $HCrO_4^-$ is mainly adsorbed on carbon surfaces [23]. The behavior of activated carbon for better adsorption at low pH may be due to the huge quantity of H^+ ions present, which neutralize the negatively charged adsorbent surface, lowering the hindrance to chromate ion diffusion [45]. As presented in Figure 2c, the pH_{PZC} of all materials ranged from 5.58 to 7.1, implying that when the solution pH decreases below these values, the surface of materials was more positively charged, and more electrostatic attraction occurred with negative ions (Cr(VI)) [46, 47]. Therefore, the highest adsorption capacity of Cr(VI) onto the surface of adsorbents was found to have the lowest pH value (pH 2), as demonstrated in Figure 3a [43]. The influence of contacting time on adsorption capacity is shown in Figure 3b, which shows that the adsorption rate rapidly increased until 180 min, then it slightly increased until 480 min. Figure 3b also indicates that the adsorption rate of chemical-modified AC was higher than that of AC, resulting in higher adsorption capacities of these materials compared with AC.

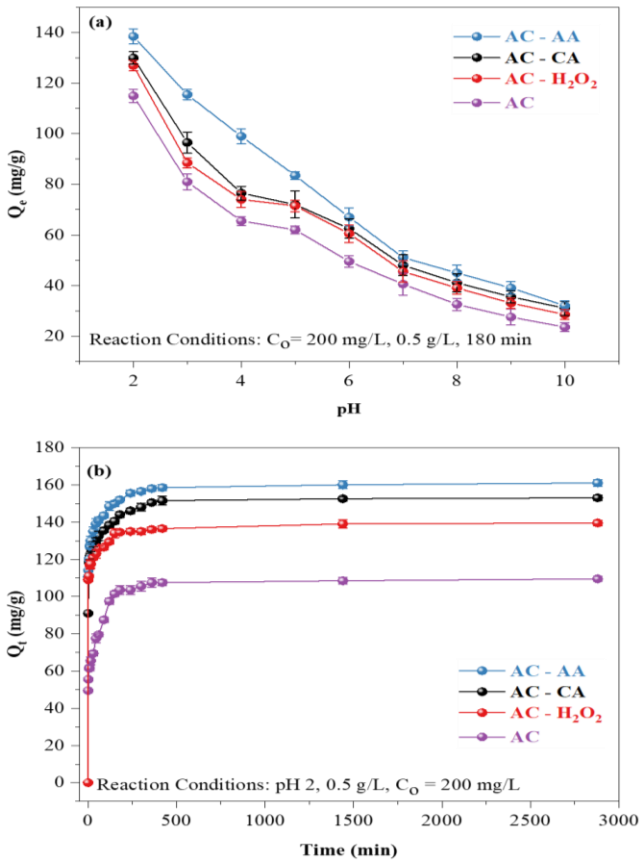

Fig. 3. Influences of the solution pH of (a) and contacting time (b).

These results might be attributed to higher functional groups, which play a crucial role in the removal of Cr (VI) [48] in chemical-modified ACs. These findings suggest that the chemical modification significantly enhances the adsorption efficiency of AC. Compared to previous studies, the equilibrium period of 180 – 360 minutes for these adsorbents is relatively shorter. The equilibrium duration of modified activated carbon created from olive bagasse was 10 hours [49], while charcoal produced from sawdust attained equilibrium in 5 hours [50], and activated carbon

synthesized from waste lignocellulosic material required 360 minutes to reach equilibrium [51]. This indicates that the chemically modified activated carbon employed in this study possesses a greater adsorption capacity and attains equilibrium more rapidly, underscoring its potential for efficient and time-effective Cr(VI) removal applications.

3.4. Adsorption isotherms

Figure 4 shows the necessary fitting result for the kinetic data for three common adsorption isotherm models, including the Langmuir, Freundlich, and Redlich-Peterson (R-P) models. The Langmuir and Freundlich models are the most common adsorption isotherms based on different assumptions related to different adsorption processes. The R-P model, a hybrid model of these two models, is more suitable for describing the actual adsorption process, usually incorporating chemical- and physical-related phenomena [52]. As illustrated in Figure 4, the R-P model is the most fitted with experimental data, indicating the combination of chemical and physical processes in the adsorption [53]. Furthermore, the g value close to 1 in the R-P model (Table S1) and the better fit of the experimental data with the Langmuir model compared to the Freundlich model suggest that chemical adsorption dominates the Cr(VI) adsorption process, which is consistent with the findings of previous studies [54-56].

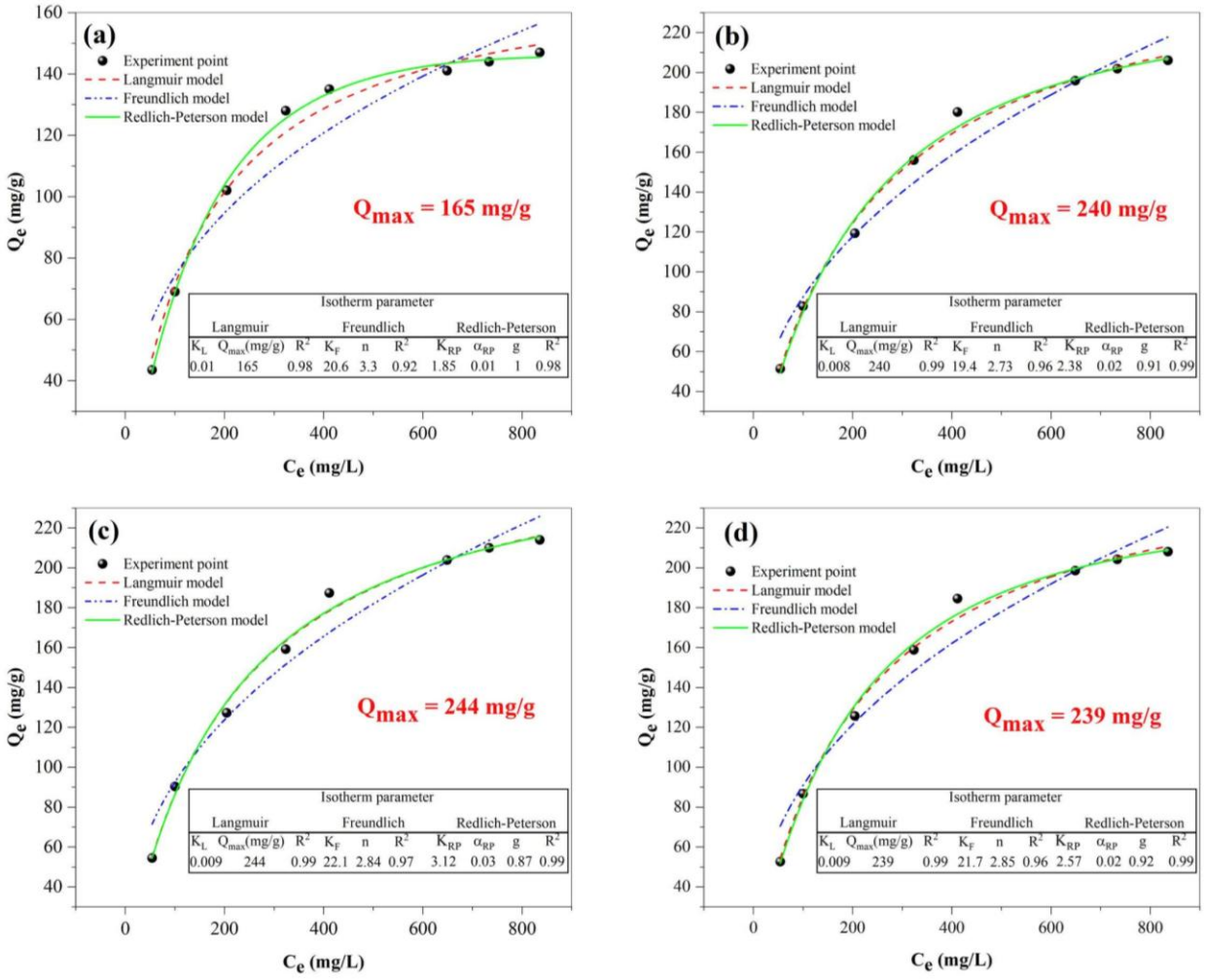

Fig. 4. Adsorption isotherms parameters of adsorbent materials for Cr(VI) adsorption of (a) AC, (b) AC-H_2O_2, (c) AC-AA, and (d) AC-CA.

The maximum adsorption capacity obtained from the Langmuir model revealed that the AC adsorption capacity was 165 mg/g, which was lower than the adsorption capacities of AC-AA (244 mg/g), AC-CA (230 mg/g), and AC-H_2O_2 (240 mg/g). The higher maximum adsorption capacities

of chemically modified ACs compared to AC can be explained by two main reasons: (1) the electrostatic interaction between the adsorbent and the adsorbate, which has been evidenced in the pH effect experiment (Figure 3a); and (2) the presence of functional groups on the surface of the materials. The enhanced adsorption performance of AC-AA is attributed to the introduction of oxygen-containing functional groups (–COOH), which increase surface polarity and provide additional interaction sites for Cr(VI) species [57]. When comparing the maximum adsorption capacity (Table S2), all materials had much higher adsorption capacities than those of other studies, such as corn straw (176 mg/g), nanotubes (85.8 mg/g), apple peels (36 mg/g), etc. The results showed that the adsorption capacities of the materials synthesized in this study were superior to those of the reported materials, even higher than those of the materials synthesized by more complicated modification processes, such as nanotubes, or using more chemicals and posing more potential risks to the environment.

3.5. Adsorption kinetics

Figure 5 illustrates the kinetic data fitting results for the PFO, PSO, and Elovich models, which were obtained using four adsorbents. All the parameters obtained from all adsorbents exhibited a better fit to the Elovich model ($R^2 > 0.95$) than those of the PFO and PSO models. These results reveal that the four materials primarily demonstrate a chemisorption mechanism associated with a diffusion-controlled process [58, 59]. Previous investigations have demonstrated Cr(VI)'s chemisorption behavior on several adsorbents [60-63]. Furthermore, the high α value of the Elovich model obtained with three chemical-modified materials indicates that the surface of these materials is highly heterogeneous [64], which might facilitate the adsorption process to obtain high adsorption capacities. The agreement between the results from adsorption isotherms and kinetics can confirm the importance of chemical reactions in the adsorption of Cr(VI) on the synthesized materials. The process might include the development of valence forces and is determined by the donation or exchange of electrons between the adsorbent and the energetically heterogeneous surface of the adsorbent [57, 65, 66].

3.6. Adsorption thermodynamics

Table 2 shows the negative values of $\Delta G°$ and positive values of $\Delta H°$ for the adsorption processes of all materials, indicating that the adsorption process is spontaneous and endothermic. Adsorption is influenced by temperature and depends on the mobility of heavy metal ions, and the $\Delta H°$ value also reveals whether or not the adsorption is being motivated by strong attraction forces [67]. The adsorption process of Cr(VI) on synthesized materials was endothermic in nature, meaning that heat was absorbed when the reaction moved forward. The positive value of $\Delta S°$ indicates an increase in reaction irregularity at the solid-liquid interface [68].

The thermodynamic data reveal variations in the effectiveness of different adsorbent materials (AC, AC-CA, AC-AA, and AC-H_2O_2) for Cr(VI) removal. At the lowest temperature (283 K), AC-H_2O_2 showed the smallest negative $\Delta G°$, indicating lower spontaneity compared to the other materials in these conditions. In contrast, AC-AA exhibited the highest negative $\Delta G°$ across all temperature points, suggesting it is the most spontaneous adsorbent for Cr(VI). Furthermore, AC-AA had the lowest $\Delta H°$, indicating a weaker endothermic reaction but still maintaining good adsorption capacity. On the other hand, AC-H_2O_2 had higher $\Delta H°$ and $\Delta S°$, indicating greater temperature dependence and a more significant increase in disorder at the adsorbent surface. While AC showed reliable performance, it generally had lower spontaneity and thermodynamic efficiency than the modified adsorbents.

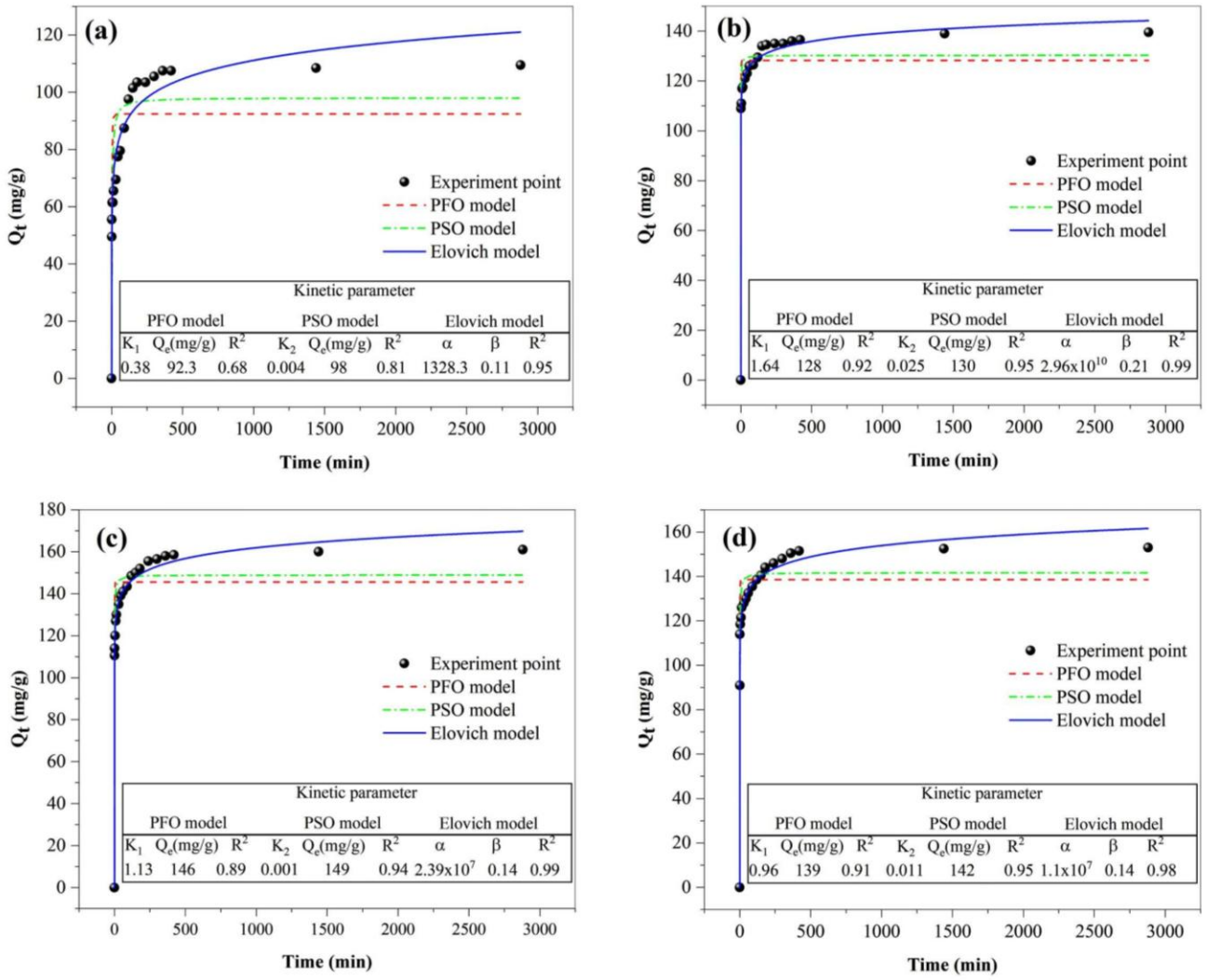

Fig. 5. Kinetic parameters for Cr(VI) adsorption of absorbent materials of (a) AC), (b) AC-H_2O_2, (c) AC-AA, and (d) AC-CA.

Table 2. Thermodynamic parameters of adsorbent materials for Cr(VI) adsorption.

Materials	Temperature (K)	ΔG° (kJ/mol)	ΔH° (kJ/mol)	ΔS° (J/mol.K)
AC	283	-23.15	2.55	90.8
	303	-24.96		
	313	-25.87		
AC-CA	283	-22.29	1.82	85.21
	303	-24.01		
	313	-24.85		
AC-AA	283	-22.33	0.8	82.72
	303	-23.96		
	313	-24.78		
AC-H_2O_2	283	-22.15	1.42	83.29
	303	-23.82		

Among the modified adsorbents, AC-AA exhibited superior performance at lower temperatures, likely due to the greater spontaneity of its adsorption process (more negative ΔG°). In contrast, AC-H_2O_2 demonstrated enhanced adsorption capacity at elevated temperatures, which could be attributed to its endothermic nature (positive ΔH°) and higher entropy gain (ΔS°). In summary, the most suitable

adsorbent depends on the specific conditions, with AC-AA being optimal at lower temperatures and AC-H_2O_2 excelling at higher temperatures.

3.7. Desorption experiments

The results in Figure 6 indicate that NaOH is the most efficient desorption agent among the three tested, whereas HCl and hot water at 60°C show comparatively lower effectiveness in releasing chromium. The use of HCl and hot water solutions is particularly ineffective in desorbing chromium.

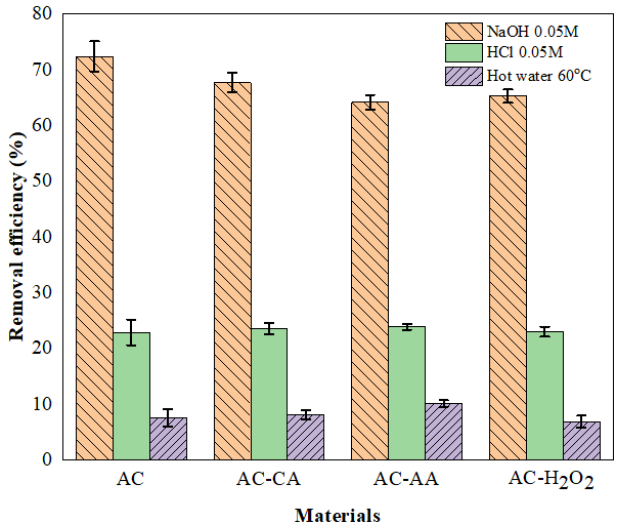

Fig. 6. Desorption efficiency of Cr(VI) on the adsorbents.

At pH values lower than the pH_{pzc}, the surface of the adsorbent carries a positive charge. This leads to an electrostatic attraction with OH^- ions from the NaOH solution, causing these ions to adhere to the surface and subsequently displacing $HCrO_4^-$ ions into the surrounding environment. Conversely, at pH levels higher than pH_{pzc}, the adsorbent surface becomes negatively charged, while Cr(VI) primarily exists as CrO_4^{2-} in alkaline conditions. Under these circumstances, the desorption of Cr(VI) is facilitated through the exchange of CrO_4^{2-} ions with OH^- ions. Notably, the experiments demonstrated that approximately 70% of Cr(VI) could be desorbed using NaOH, indicating that electrostatic forces play a key role in the adsorption of Cr(VI) [69-71]. In this case, the surface adsorbent charge was positively charged, so using a base to compete with $HCrO_4^-$ anions was an effective desorption selection. Moreover, the adsorption mechanism of AC appears to rely predominantly on physical interactions, whereas chemical adsorption processes contribute more significantly to other types of materials.

Both methods have significant limitations when using HCl and hot water at 60°C for chromium desorption. HCl creates an acidic environment that facilitates chromium desorption, but its efficiency is hindered as chromium typically exists as Cr^{3+} or forms insoluble complexes in such conditions, preventing complete release from the adsorbent. Furthermore, HCl is unable to oxidize chromium to the more soluble Cr(VI) form, limiting the desorption process. Hot water exhibits the lowest desorption efficiency compared to the other methods. As the temperature increases, thermal energy intensifies molecular vibrations, enhancing interactions between water molecules and the adsorbent surface [72]. This agitation can only break the weakest physical bonds, allowing for the partial release of ions into the environment. These findings indicate that weak intermolecular forces, such as van der Waals or gravitational interactions, contribute to the adsorption mechanisms of all materials.

3.8. Effect of NaCl and the various sources

Wastewater from different industries contains a variety of salts, and their presence results in high ionic strength, which could have a negative impact on the effectiveness of the adsorption process [73]. The research results presented in Figure 7a showed that the chromium adsorbent solution's adsorption capacity varied when NaCl was added, significantly influencing the chromium adsorption capacity of the adsorbent. Chromium could adsorb more slowly on the adsorbent when Cl^- ions were present. In comparison, with the absence of Cl^-, the concentration of Cl^- increased from 0.01 M to 1 M. The following includes the explanations for this phenomenon: (1) The adsorbent surface was positively charged at pH 2, which caused the Cl^- ion to compete with $HCrO_4^-$ in the adsorption process on the adsorbent surface, causing the adsorption capacity to gradually decrease with increasing Cl^- ion concentrations.

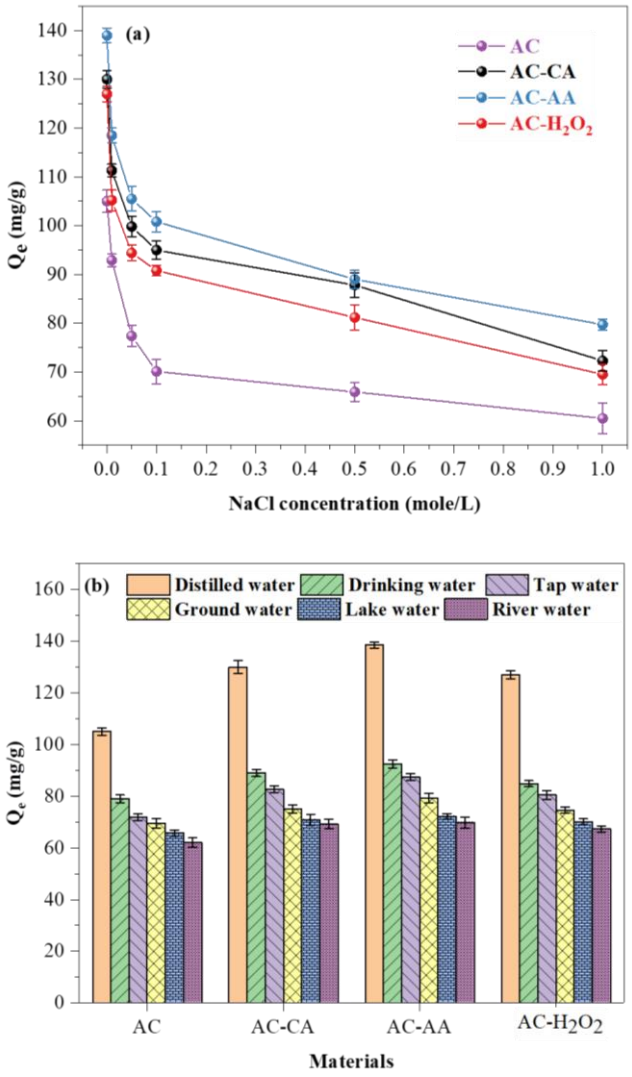

Fig. 7. Effect of ion strength NaCl concentration (a) and influence of different water sources (b) on adsorption capacity (Under conditions: C_o = 200 mg/L, 3h, pH 2, solid/liquid ratio 0.5g/L, at room temperature).

Because the higher the concentration of NaCl, the more Cl^- ions were present in the solution, increasing the competition with $HCrO_4^-$ in the adsorption process; (2) High NaCl concentrations may increase the ionic strength of the solution, which may affect the Cr(VI) activity coefficient and significantly lessen collision and contact between the sorbent [74]; (3) The adsorbent species in solution come into contact with the solid adsorbent; these species are encircled by an electrically diffused double layer, and the thickness of which is noticeably increased by the addition of NaCl. Due to a decrease in electrostatic attraction caused by this expansion, the amount of Cr(VI) ions that may be absorbed is also reduced. This expansion prevents the adsorbent particles and Cr(VI) species from interacting intimately with one another [75]. The adsorption process was significantly impacted by substances from water sources, as shown in Figure 7b. For all materials, the adsorption capacity decreased in the following order: distilled water > drinking water > tap water > ground water > lake water > river water. The order in which this adsorbent's adsorption capacity was reduced corresponds exactly to the quality of the water: distilled water > drinking water > tap water > groundwater > lake water > river water. It was shown that the dissolved su in the environment possessed significant competitive influence and reduced the adsorption capacity in particular water environments. The higher the water quality, the greater the ion competition between them. An insignificant amount of $HCrO_4^-$ was present in water that contained ions. On the contrary, the amount of the different ions in the water source increases with reduced water quality, increasing the competition with $HCrO_4^-$ in the case of lake and river water.

3.9. Proposed mechanisms

Hexavalent and trivalent chromium may coexist in the solution and on the adsorbent after the Cr(VI) adsorption procedure if the reduction of Cr(VI) to Cr(III) takes place. Many researchers have looked into the errors made when chromium species were analyzed in aqueous environments (liquid phase) and on the laden adsorbent (solid phase) following the Cr(VI) adsorption procedure [76]. Basically, atomic absorption spectroscopy (AAS) is used to determine the total (trivalent and hexavalent) chromium in solution [44]. The reduction of Cr(VI) may be partially attributed to electron-donating surface functionalities, particularly phenolic groups, in acidic conditions [77]. Figure 8 shows these results, as protons were utilized during Cr(VI) reduction, the reduction rate of Cr(VI) increased with decreasing solution pH [78].

This is also possible to remove Cr(VI) at low pH levels thanks to the emergence of two "indirect" mechanisms [33]. The initial mechanism is when functional groups on the adsorbent's surface that act as electron donor groups come into contact with Cr(VI) in solution, the more toxic Cr(VI) is reduced to less hazardous Cr(III). This is because

Cr(VI) exhibits a strong redox (typically greater than +1.35V) under normal circumstances.

According to the literature, when Cr(VI) oxyanions interact with the electron-donating groups of the adsorbent (such as hydroxyl groups), Cr(VI) is spontaneously reduced to Cr(III) [44]. The functional groups on the material's surface that contain oxygen provide the e- in the Equation (13). The second mechanism includes a three-step procedure: (i) The association of Cr(VI) anions with positively charged groups on the surface of the material; (ii) Conversion of Cr(VI) to Cr(III) by adjacent electron donor groups in the Equation (14); (iii) Release of Cr(III) cations into the aqueous phase due to electrostatic repulsion between positively charged groups and Cr(III) cations, or complexation of Cr(III) with neighboring functional groups in the Equations (15) and (16).

Based on the above mechanisms and results, it has been shown that the adsorption process of the adsorbent is mostly Cr(VI).

The researchers showed that a portion of Cr(VI) anions underwent reduction to Cr(III) cations. Throughout this process, the abundant hydroxyl groups present on the surface of activated carbon played a crucial role in donating electrons.

$$HCrO_4^- + 7H^+ + 3e^- \Leftrightarrow Cr^{3+} + 4H_2O \ (E° = + 1.35V) \quad (13)$$

$$3Cx\text{-}OH + HCrO_4^- + 4H^+ + 3e^- \Leftrightarrow 3Cx\text{-}O^- + Cr^{3+} + 4H_2O \ (E° = + 1.35\ V) \quad (14)$$

$$2Cx\text{-}CO^- + Cr^{3+} \Leftrightarrow [(Cx\text{-}CO)_2Cr]^+ \quad (15)$$

$$2Cx\text{-}OH_2^+ + Cr^{3+} \Leftrightarrow [(Cx\text{-}CO)_2Cr]^+ + 2H^+ \quad (16)$$

Moreover, adsorbents with a high surface area enhance the adsorption process by providing more sites for chromium to interact with, particularly on the pore surface.

Therefore, the mechanism of chromium adsorption onto the material primarily occurs at the surface level. In addition, reaction conditions at low pH will show pH < pH_{pzc}, the charge surface of the material will carry a positive charge that mainly results from the OH_2^+ groups present on its structure.

Therefore, electrostatic attraction between the OH_2^+ groups and Cr(VI) anions in solution. This is considered one of the mechanisms contributing to chromium removal in this study.

Based on the analysis of the characteristics and results obtained from the experimental investigations, the adsorption mechanisms of Cr(VI) onto the absorbent in this study are depicted in Figure 9. Besides the chemical adsorption mechanism, the physical adsorption mechanism is also important due to electrostatic interaction.

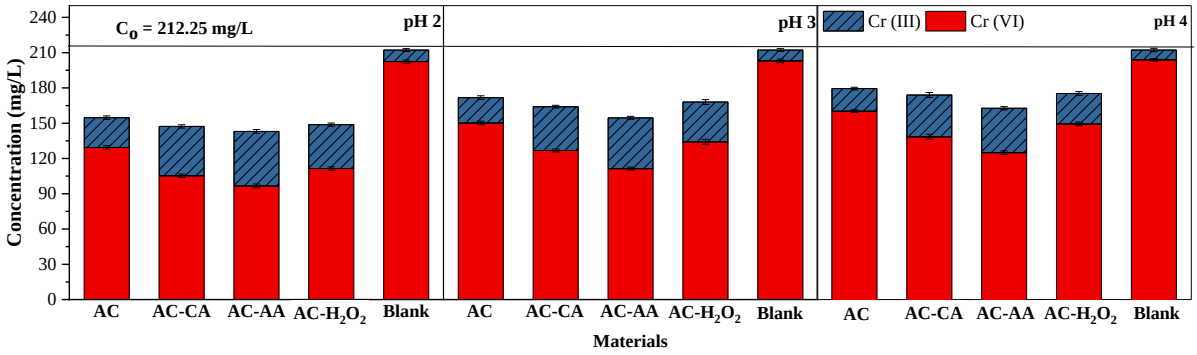

Fig. 8. The concentration after adsorption of Cr(VI) – Cr(III) for separate adsorption experiments of all materials.

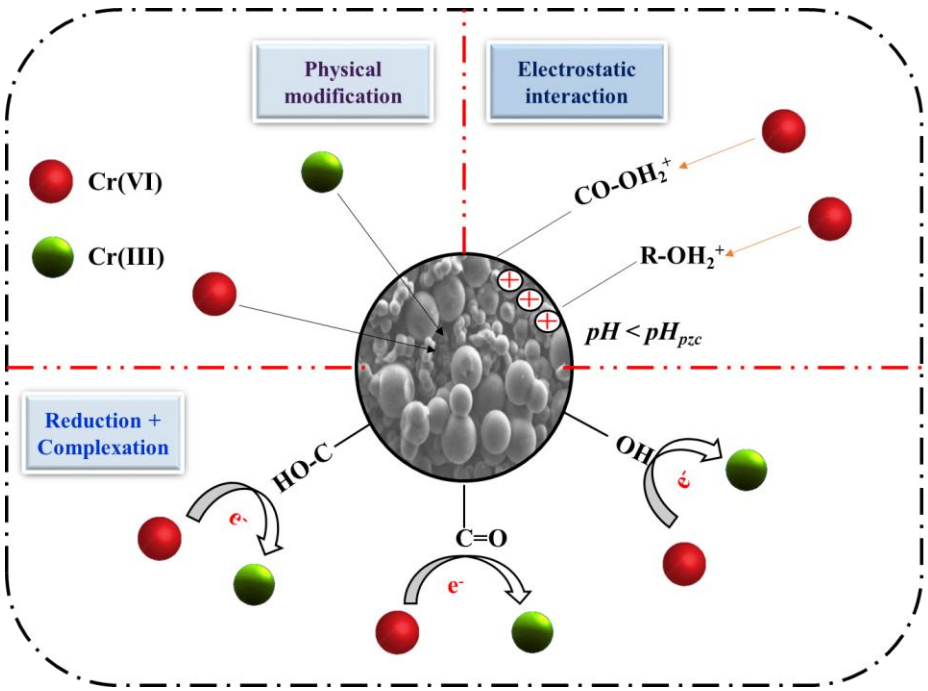

Fig. 9. The adsorption mechanisms of absorbent.

Furthermore, desorption experiments have shown that AC is most effective in desorbing when treated with NaOH. This suggests that AC has a low number of functional groups, so the physical mechanism plays a more dominant role than the chemical mechanism. In addition, for materials modified with different chemicals, these materials will have varying numbers of functional groups present on their surfaces (e.g., protonated carboxylic and phenolic moieties). This enhances the chemical mechanism of these materials, increasing their chromium adsorption capacity in solution. Moreover, the adsorbed Cr(VI) could be partly reduced to Cr(III) with the electron donor provided by the oxygen-containing functional groups. Next, complexation between Cr(VI) and oxygen-containing functional groups. Lastly, chromium ions could be trapped in the micropores on the absorbent surface.

4. Conclusion

In this study, materials synthesized from spherical hydrothermal hydrochar, combined with chemical impregnation using H_2O_2, CA, and AA, followed by pyrolysis, were employed to adsorb Cr(VI) from aqueous solutions. The adsorption mechanism was explored through investigations into the effects of adsorption conditions, as well as the kinetics and thermodynamics of the process.

The results indicated that chemical impregnation in the synthesizing process significantly improved the adsorption capacity at pH 2, which might be due to the higher functional groups in these materials.

The kinetic study indicated that the Elovich model was the best model fit to the experimental data of all materials, implying the chemical mechanism governing the adsorption process. Thermodynamic assessments demonstrated that Cr(VI) adsorption was spontaneous ($\Delta G<0$), endothermic ($\Delta H>0$), and entropy-favored ($\Delta S>0$). Desorption experiments revealed that NaOH 0.05M was the best solution for the desorption of Cr(VI). Different NaCl and background solutions experiments indicated that ion strength and soluble contents could reduce the adsorption capacity. The adsorption mechanisms included electrostatic interaction, reduction, and complexation. This study provides insights to better understand the mechanisms and factors influencing Cr(VI) adsorption; the experiments demonstrate that impregnating biochar with familiar chemicals before hydrolysis can enhance its adsorption capacity.

Acknowledgements

The authors would like to express their gratitude to Ms. Nguyen Thi Phuong and Ms. Nguyen Thi Cam Vi for their assistance in conducting the experiments.

Author's contribution

Conceptualization: Nguyen Duy Dat; Methodology: Nguyen Duy Dat; Formal analysis and investigation: Nguyen Duy Dat, Quang Sang Huynh; Writing - original draft preparation: Quang Sang Huynh, Nguyen Duy Dat; Writing - review and editing: Nguyen Duy Dat, My Linh Nguyen; Supervision: Nguyen Duy Dat.

Conflict of interest

No potential conflict of interest was reported by the authors.

Data availability

The datasets generated and/or analyzed during the current study are available from the corresponding author on reasonable request.

Funding

Self-funded.

Declaration of Using Generative AI

Generative AI was used solely for improving readability and language editing. The authors take full responsibility for the content and interpretation of the manuscript

References

[1] Dat, N. D., Nguyen, L. S. P., Vo, T.-D.-H., Van Nguyen, T., Do, T. T. L., Tran, A. T. K., & Hoang, N. T.-T. (2023). Pollution characteristics, associated risks, and possible sources of heavy metals in road dust collected from different areas of a metropolis in Vietnam. *Environmental Geochemistry and Health*, *45*, 7889-7907. https://doi.org/10.1007/s10653-023-01696-4

[2] Dat, N. D., Huynh, Q. S., Tran, K. A. T., & Nguyen, M. L. (2023). Performance of heterogeneous Fenton catalyst from solid wastes for removal of emerging contaminant in water: A potential approach to circular economy. *Results in Engineering*, *18*, 101086. https://doi.org/10.1016/j.rineng.2023.101086

[3] Cataldo, E., Salvi, L., Paoli, F., Fucile, M., Masciandaro, G., Manzi, D., Masini, C. M., & Mattii, G. B. (2021). Application of zeolites in agriculture and other potential uses: A review. *Agronomy*, *11*, 1547. https://doi.org/10.3390/agronomy11081547

[4] Valentín-Reyes, J., García-Reyes, R., García-González, A., Soto-Regalado, E., & Cerino-Córdova, F. (2019). Adsorption mechanisms of hexavalent chromium from aqueous solutions on modified activated carbons. *Journal of Environmental Management*, *236*, 815-822. https://doi.org/10.1016/j.jenvman.2019.02.014

[5] Dhar, P. K., Naznin, A., & Hosna Ara, M. (2020). Health risks assessment of heavy metal contamination in drinking water collected from different educational institutions of Khulna City Corporation, Bangladesh. *Advances in Environmental Technology*, *4*, 235–250.

[6] Ali, H., Khan, E., & Ilahi, I. (2019). Environmental chemistry and ecotoxicology of hazardous heavy metals: Environmental persistence, toxicity, and bioaccumulation. *Journal of Chemistry*, *2019*, 6730305. https://doi.org/10.1155/2019/6730305

[7] den Braver-Sewradj, S. P., van Benthem, J., Staal, Y. C., Ezendam, J., Piersma, A. H., & Hessel, E. V. (2021). Occupational exposure to hexavalent chromium. Part II. Hazard assessment of carcinogenic effects. *Regulatory Toxicology and Pharmacology*, *126*, 105045. https://doi.org/10.1016/j.yrtph.2021.105045

[8] Boosaeidi, N., Pourkhabbaz, A., & Jahani, M. (2017). Biosorption of hexavalent chromium by the agricultural wastes of the cotton and barberry plants. *Advances in Environmental Technology*, *3*(3), 159–167. https://doi.org/10.22104/aet.2017.579

[9] Achmad, R. T., & Auerkari, E. I. (2017). Effects of chromium on human body. *Annual Research & Review in Biology*, *13*, 1-8. https://doi.org/10.9734/ARRB/2017/33462

[10] World Health Organization. (2020). *Chromium in drinking-water*. World Health Organization.

[11] Sinduja, M., Sathya, V., Maheswari, M., Dhevagi, P., Kalpana, P., Dinesh, G., & Prasad,

S. (2022). Evaluation and speciation of heavy metals in the soil of the sub urban region of Southern India. *Soil and Sediment Contamination*, *31*, 974-993. https://doi.org/10.1080/15320383.2022.2030298

[12] Velusamy, S., Roy, A., Sundaram, S., & Kumar Mallick, T. (2021). A review on heavy metal ions and containing dyes removal through graphene oxide-based adsorption strategies for textile wastewater treatment. *The Chemical Record*, *21*, 1570-1610. https://doi.org/10.1002/tcr.202000153

[13] Phạm, H. G., & Đỗ, Q. H. (2016). Nghiên cứu xử lý kim loại nặng trong nước bằng phương pháp hấp phụ trên phụ phẩm nông nghiệp biến tính axit photphoric. VNU *Journal of Science: Earth and Environmental Sciences*, *32*(1). https://js.vnu.edu.vn/EES/article/view/2686

[14] Vo, A. T., Nguyen, V. P., Ouakouak, A., Nieva, A., Doma Jr, B. T., Tran, H. N., & Chao, H.-P. (2019). Efficient removal of Cr(VI) from water by biochar and activated carbon prepared through hydrothermal carbonization and pyrolysis: Adsorption-coupled reduction mechanism. *Water*, *11*, 1164. https://doi.org/10.3390/w11061164

[15] Ma, H., Yang, J., Gao, X., Liu, Z., Liu, X., & Xu, Z. (2019). Removal of chromium(VI) from water by porous carbon derived from corn straw: Influencing factors, regeneration and mechanism. *Journal of Hazardous Materials*, *369*, 550-560. https://doi.org/10.1016/j.jhazmat.2019.02.063

[16] Enniya, I., Rghioui, L., & Jourani, A. (2018). Adsorption of hexavalent chromium in aqueous solution on activated carbon prepared from apple peels. *Sustainable Chemistry and Pharmacy*, *7*, 9-16. https://doi.org/10.1016/j.scp.2017.11.003

[17] Demiral, İ., Samdan, C., & Demiral, H. (2021). Enrichment of the surface functional groups of activated carbon by modification method. *Surfaces and Interfaces*, *22*, 100873. https://doi.org/10.1016/j.surfin.2020.100873

[18] Danish, M., Pin, Z., Ziyang, L., Ahmad, T., Majeed, S., Yahya, A. N. A., Khanday, W. A., & Khalil, H. A. (2022). Preparation and characterization of banana trunk activated carbon using H3PO4 activation: A rotatable central composite design approach. *Materials Chemistry and Physics*, *282*, 125989. https://doi.org/10.1016/j.matchemphys.2022.125989

[19] Li, D., Guo, Y., Li, Y., Liu, Z., & Chen, Z. (2022). Waste-biomass tar functionalized carbon spheres with N/P Co-doping and hierarchical pores as sustainable low-cost energy storage materials. *Renewable Energy*, *188*, 61-69. https://doi.org/10.1016/j.renene.2022.01.109

[20] An, Q., Wang, Q., & Zhai, J. (2024). Hydrothermal carbonization of corncob for hydrochar production and its combustion reactivity in a blast furnace. *Environmental Science and Pollution Research*, *31*, 16653-16666. https://doi.org/10.1007/s11356-024-32242-z

[21] Nizamuddin, S., Baloch, H. A., Griffin, G. J., Mubarak, N. M., Bhutto, A. W., Abro, R., Mazari, S. A., & Ali, B. S. (2017). An overview of effect of process parameters on hydrothermal carbonization of biomass. *Renewable and Sustainable Energy Reviews*, *73*, 1289-1299. https://doi.org/10.1016/j.rser.2016.12.122

[22] Li, M., Li, W., & Liu, S. (2011). Hydrothermal synthesis, characterization, and KOH activation of carbon spheres from glucose. *Carbohydrate Research*, *346*, 999-1004. https://doi.org/10.1016/j.carres.2011.03.020

[23] Kumar, A., & Jena, H. M. (2017). Adsorption of Cr(VI) from aqueous solution by prepared high surface area activated carbon from Fox nutshell by chemical activation with H3PO4. *Journal of Environmental Chemical Engineering*, *5*, 2032-2041. https://doi.org/10.1016/j.jece.2017.03.035

[24] Liu, X., He, C., Yu, X., Bai, Y., Ye, L., Wang, B., & Zhang, L. (2018). Net-like porous activated carbon materials from shrimp shell by solution-processed carbonization and H3PO4 activation for methylene blue adsorption. *Powder Technology*, *326*, 181-189. https://doi.org/10.1016/j.powtec.2017.12.034

[25] Shi, Y., Liu, G., Wang, L., & Zhang, H. (2019). Activated carbons derived from hydrothermal impregnation of sucrose with phosphoric acid: Remarkable adsorbents for sulfamethoxazole removal. *RSC Advances*, *9*, 17841-17851. https://doi.org/10.1039/C9RA02610J

[26] Wang, Y., Xu, Y., Lu, X., Liu, K., Li, F., Wang, B., Wang, Q., Zhang, X., Yang, G., & Chen, J. (2023). Biomass-based hydrothermal carbons for the contaminants removal of wastewater: A mini-review. *International Journal of Molecular Sciences*, *24*, 1769. https://doi.org/10.3390/ijms24021769

[27] Bedin, K. C., Martins, A. C., Cazetta, A. L., Pezoti, O., & Almeida, V. C. (2016). KOH-activated carbon prepared from sucrose spherical carbon: Adsorption equilibrium, kinetic and thermodynamic studies for methylene blue removal. *Chemical Engineering Journal*, *286*, 476-484. https://doi.org/10.1016/j.cej.2015.10.099

[28] Kim, D.-W., Kil, H.-S., Nakabayashi, K., Yoon, S.-H., & Miyawaki, J. (2017). Structural elucidation of physical and chemical activation mechanisms based on the microdomain structure model. *Carbon*, *114*, 98-105. https://doi.org/10.1016/j.carbon.2016.11.082

[29] Zhang, P., Qiao, Z.-A., & Dai, S. (2015). Recent advances in carbon nanospheres: Synthetic routes and applications. *Chemical Communications*, *51*, 9246-9256. https://doi.org/10.1039/C5CC01759A

[30] Tran, H. N., Lee, C.-K., Nguyen, T. V., & Chao, H.-P. (2018). Saccharide-derived microporous spherical biochar prepared from hydrothermal carbonization and different pyrolysis temperatures: Synthesis, characterization, and application in water treatment. *Environmental Technology*, *39*, 2747-2760. https://doi.org/10.1080/09593330.2017.1365941

[31] Schumacher, P., Fischer, F., Sann, J., Walter, D., & Hartwig, A. (2022). Impact of nano- and micro-sized chromium(III) particles on cytotoxicity and gene expression profiles related to genomic stability in human keratinocytes and alveolar epithelial cells. *Nanomaterials*, *12*, 1294. https://doi.org/10.3390/nano12081294

[32] Zhao, J., Yu, L., Ma, H., Zhou, F., Yang, K., & Wu, G. (2020). Corn stalk-based activated carbon synthesized by a novel activation method for high-performance adsorption of hexavalent chromium in aqueous solutions. *Journal of Colloid and Interface Science*, *578*, 650-659. https://doi.org/10.1016/j.jcis.2020.06.031

[33] Tran, H. N., You, S.-J., Hosseini-Bandegharaei, A., & Chao, H.-P. (2017). Mistakes and inconsistencies regarding adsorption of contaminants from aqueous solutions: A critical review. *Water Research*, *120*, 88-116. https://doi.org/10.1016/j.watres.2017.04.014

[34] Tran, H. N., You, S.-J., & Chao, H.-P. (2016). Thermodynamic parameters of cadmium adsorption onto orange peel calculated from various methods: A comparison study. *Journal of Environmental Chemical Engineering*, *4*, 2671-2682. https://doi.org/10.1016/j.jece.2016.05.009

[35] Tran, H. N., Chao, H.-P., & You, S.-J. (2018). Activated carbons from golden shower upon different chemical activation methods: Synthesis and characterizations. *Adsorption Science & Technology*, *36*, 95-113. https://doi.org/10.1177/0263617416684837

[36] Pakade, V. E., Madikizela, L. M., Klink, M. J., & Ncube, S. (2023). Adsorption of toxic heavy metals using charred and uncharred coffee waste adsorbents: A review. *Environmental Technology Reviews*, *12*, 359-389. https://doi.org/10.1080/21622515.2023.2215459

[37] Kirishnamaline, G., Magdaline, J. D., Chithambarathanu, T., Aruldhas, D., & Anuf, A. R. (2021). Theoretical investigation of structure, anticancer activity and molecular docking of thiourea derivatives. *Journal of Molecular Structure*, *1225*, 129118. https://doi.org/10.1016/j.molstruc.2020.129118

[38] Vu, N.-T., & Do, K.-U. (2023). Insights into adsorption of ammonium by biochar derived from low temperature pyrolysis of coffee husk. *Biomass Conversion and Biorefinery*, *13*, 2193-2205. https://doi.org/10.1007/s13399-021-01337-9

[39] Liu, X., Renard, C. M., Bureau, S., & Le Bourvellec, C. (2021). Revisiting the contribution of ATR-FTIR spectroscopy to characterize plant cell wall polysaccharides. *Carbohydrate Polymers*, *262*, 117935. https://doi.org/10.1016/j.carbpol.2021.117935

[40] Zhao, N., Zhao, C., Tsang, D. C., Liu, K., Zhu, L., Zhang, W., Zhang, J., Tang, Y., & Qiu, R. (2021). Microscopic mechanism about the selective adsorption of Cr(VI) from salt solution on O-rich and N-rich biochars. *Journal of Hazardous Materials*, *404*, 124162. https://doi.org/10.1016/j.jhazmat.2020.124162

[41] Liu, C., Jin, R.-N., Ouyang, X.-k., & Wang, Y.-G. (2017). Adsorption behavior of carboxylated cellulose nanocrystal—polyethyleneimine composite for removal of Cr(VI) ions. *Applied Surface Science*, *408*, 77-87. https://doi.org/10.1016/j.apsusc.2017.02.265

[42] Long, X. l., Chen, P. y., & Jin, X. y. (2024). Effect of modification with hydrobromic acid on the performance of activated carbon in the removal of hexavalent chromium from aqueous solution. *Environmental Progress & Sustainable Energy*, *43*, e14245. https://doi.org/10.1002/ep.14245

[43] Chen, M., He, F., Hu, D., Bao, C., & Huang, Q. (2020). Broadened operating pH range for adsorption/reduction of aqueous Cr(VI) using biochar from directly treated jute (Corchorus capsularis L.) fibers by H3PO4. *Chemical Engineering Journal*, *381*, 122739. https://doi.org/10.1016/j.cej.2019.122739

[44] Tran, H. N., Nguyen, D. T., Le, G. T., Tomul, F., Lima, E. C., Woo, S. H., Sarmah, A. K., Nguyen, H. Q., Nguyen, P. T., & Nguyen, D. D. (2019). Adsorption mechanism of hexavalent chromium onto layered double hydroxides-based adsorbents: A systematic in-depth review. *Journal of Hazardous Materials*, *373*, 258-270. https://doi.org/10.1016/j.jhazmat.2019.03.018

[45] Gholipour, M., Hashemipour, H., & Mollashahi, M. (2011). Hexavalent chromium removal from aqueous solution via adsorption on granular activated carbon: Adsorption, desorption, modeling and simulation studies. *Journal of Engineering and Applied Sciences*, *6*, 10-18.

[46] Lin, C., Luo, W., Luo, T., Zhou, Q., Li, H., & Jing, L. (2018). A study on adsorption of Cr(VI) by modified rice straw: Characteristics, performances and mechanism. *Journal of Cleaner Production*, *196*, 626-634. https://doi.org/10.1016/j.jclepro.2018.05.279

[47] Wu, J., Yan, X., Li, L., Gu, J., Zhang, T., Tian, L., Su, X., & Lin, Z. (2021). High-efficiency adsorption of Cr(VI) and RhB by hierarchical porous carbon prepared from coal gangue. *Chemosphere*, *275*, 130008. https://doi.org/10.1016/j.chemosphere.2021.130008

[48] Zhou, H., & Chen, Y. (2010). Effect of acidic surface functional groups on Cr(VI) removal by activated carbon from aqueous solution. *Rare Metals*, *29*, 333-338. https://doi.org/10.1007/s12598-010-0059-6

[49] Demiral, H., Demiral, I., Tümsek, F., & Karabacakoğlu, B. (2008). Adsorption of chromium(VI) from aqueous solution by activated carbon derived from olive bagasse and applicability of different adsorption models. *Chemical Engineering Journal*, *144*, 188-196. https://doi.org/10.1016/j.cej.2008.01.020

[50] Zhang, X., Zhang, L., & Li, A. (2018). Eucalyptus sawdust derived biochar generated by combining the hydrothermal carbonization and low concentration KOH modification for hexavalent chromium removal. *Journal of Environmental Management*, *206*, 989-998. https://doi.org/10.1016/j.jenvman.2017.11.079

[51] Labied, R., Benturki, O., Eddine Hamitouche, A. Y., & Donnot, A. (2018). Adsorption of hexavalent chromium by activated carbon obtained from a waste lignocellulosic material (Ziziphus jujuba cores): Kinetic, equilibrium, and thermodynamic study. *Adsorption Science & Technology*, *36*, 1066-1099. https://doi.org/10.1177/0263617417750739

[52] Lima, É. C., Adebayo, M. A., & Machado, F. M. (2015). Kinetic and equilibrium models of adsorption. In *Carbon nanomaterials as adsorbents for environmental and biological applications* (pp. 33-69). Springer.

[53] Wang, J., & Guo, X. (2020). Adsorption isotherm models: Classification, physical meaning, application and solving method. *Chemosphere*, *258*, 127279. https://doi.org/10.1016/j.chemosphere.2020.127279

[54] Cao, Y., Dong, S., Dai, Z., Zhu, L., Xiao, T., Zhang, X., Yin, S., & Soltanian, M. R. (2021). Adsorption model identification for

chromium(VI) transport in unconsolidated sediments. *Journal of Hydrology*, *598*, 126228. https://doi.org/10.1016/j.jhydrol.2021.126228

[55] Jiang, F., Wei, C., Yu, Z., Ji, L., Liu, M., Cao, Q., Wu, L., & Li, F. (2023). Fabrication of iron-containing biochar by one-step ball milling for Cr(VI) and tetracycline removal from wastewater. *Langmuir*, *39*, 18958-18970. https://doi.org/10.1021/acs.langmuir.3c02885

[56] Wu, Z., Zhang, H., Ali, E., Shahab, A., Huang, H., Ullah, H., & Zeng, H. (2023). Synthesis of novel magnetic activated carbon for effective Cr(VI) removal via synergistic adsorption and chemical reduction. *Environmental Technology & Innovation*, *30*, 103092. https://doi.org/10.1016/j.envres.2022.114616

[57] Liu, L., Cai, W., Dang, C., Han, B., Chen, Y., Yi, R., Fan, J., Zhou, J., & Wei, J. (2020). One-step vapor-phase assisted hydrothermal synthesis of functionalized carbons: Effects of surface groups on their physicochemical properties and adsorption performance for Cr(VI). *Applied Surface Science*, *528*, 146984. https://doi.org/10.1016/j.apsusc.2020.146984

[58] Khosravi, R., Moussavi, G., Ghaneian, M. T., Ehrampoush, M. H., Barikbin, B., Ebrahimi, A. A., & Sharifzadeh, G. (2018). Chromium adsorption from aqueous solution using novel green nanocomposite: Adsorbent characterization, isotherm, kinetic and thermodynamic investigation. *Journal of Molecular Liquids*, *256*, 163-174. https://doi.org/10.1016/j.molliq.2018.02.033

[59] Sodkouieh, S. M., Kalantari, M., & Shamspur, T. (2023). Methylene blue adsorption by wheat straw-based adsorbents: Study of adsorption kinetics and isotherms. *Korean Journal of Chemical Engineering*, *40*, 873-881. https://doi.org/10.1007/s11814-022-1230-0

[60] Akram, M., Bhatti, H. N., Iqbal, M., Noreen, S., & Sadaf, S. (2017). Biocomposite efficiency for Cr(VI) adsorption: Kinetic, equilibrium and thermodynamics studies. *Journal of Environmental Chemical Engineering*, *5*, 400-411. https://doi.org/10.1016/j.jece.2016.12.002

[61] Islam, M. A., Angove, M. J., & Morton, D. W. (2019). Recent innovative research on chromium(VI) adsorption mechanism. *Environmental Nanotechnology, Monitoring & Management*, *12*, 100267. https://doi.org/10.1016/j.enmm.2019.100267

[62] Liu, W., Zhang, J., Zhang, C., Wang, Y., & Li, Y. (2010). Adsorptive removal of Cr(VI) by Fe-modified activated carbon prepared from Trapa natans husk. *Chemical Engineering Journal*, *162*, 677-684. https://doi.org/10.1016/j.cej.2010.06.020

[63] Luo, T., Xing, X., Zhang, X., Yue, W., & Ma, X. (2023). Efficient adsorption on Cr(VI) and electrochemical application of N, P co-doped carbon spheres. *Korean Journal of Chemical Engineering*, *40*, 2826-2838. https://doi.org/10.1007/s11814-023-1514-z

[64] Pamidimukkala, P. S., & Soni, H. (2018). Efficient removal of organic pollutants with activated carbon derived from palm shell: Spectroscopic characterisation and experimental optimisation. *Journal of Environmental Chemical Engineering*, *6*, 3135-3149. https://doi.org/10.1016/j.jece.2018.04.013

[65] Chen, Q., & Wu, Q. (2015). Preparation of carbon microspheres decorated with silver nanoparticles and their ability to remove dyes from aqueous solution. *Journal of Hazardous Materials*, *283*, 193-201. https://doi.org/10.1016/j.jhazmat.2014.09.024

[66] Nguyen, V.-T., Dat, N. D., Do, Q.-H., Le, V.-A., Truong, Q.-M., Nguyen, T.-B., Tran, A. T. K., Nguyen, M. L., Hoang, N. T.-T., & My, T. T. A. (2024). Modified sucrose biochar goethite (α-FeOOH): A potential adsorbent for methylene blue removal. *Korean Journal of Chemical Engineering*, 1-12. https://doi.org/10.1007/s11814-024-00237-8

[67] González-López, M. E., Laureano-Anzaldo, C. M., Pérez-Fonseca, A. A., Arellano, M., & Robledo-Ortíz, J. R. (2021). Chemically modified polysaccharides for hexavalent chromium adsorption. *Separation and Purification Reviews*, *50*, 333-362. https://doi.org/10.1080/15422119.2020.1783311

[68] Babapour, M., Dehghani, M. H., Alimohammadi, M., Arjmand, M. M., Salari, M., Rasuli, L., Mubarak, N. M., & Khan, N. A. (2022). Adsorption of Cr(VI) from aqueous solution using mesoporous metal-organic

framework-5 functionalized with the amino acids: Characterization, optimization, linear and nonlinear kinetic models. *Journal of Molecular Liquids*, *345*, 117835. https://doi.org/10.1016/j.molliq.2021.117835

[69] Daneshvar, E., Zarrinmehr, M. J., Kousha, M., Hashtjin, A. M., Saratale, G. D., Maiti, A., Vithanage, M., & Bhatnagar, A. (2019). Hexavalent chromium removal from water by microalgal-based materials: Adsorption, desorption and recovery studies. *Bioresource Technology*, *293*, 122064. https://doi.org/10.1016/j.biortech.2019.122064

[70] Santhosh, C., Daneshvar, E., Tripathi, K. M., Baltrėnas, P., Kim, T., Baltrėnaitė, E., & Bhatnagar, A. (2020). Synthesis and characterization of magnetic biochar adsorbents for the removal of Cr(VI) and acid orange 7 dye from aqueous solution. *Environmental Science and Pollution Research International*, *27*, 32874-32887. https://doi.org/10.1007/s11356-020-09275-1

[71] Sun, Z., Liu, B., Li, M., Li, C., & Zheng, S. (2020). Carboxyl-rich carbon nanocomposite based on natural diatomite as adsorbent for efficient removal of Cr(VI). *Journal of Materials Research and Technology*, *9*, 948-959. https://doi.org/10.1016/j.jmrt.2019.11.034

[72] Zhang, B., Zhu, Z., Wang, X., Liu, X., & Kapteijn, F. (2024). Water adsorption in MOFs: Structures and applications. *Advanced Functional Materials*, *34*, 2304788. https://doi.org/10.1002/adfm.202304788

[73] Castro-Castro, J. D., Macías-Quiroga, I. F., Giraldo-Gómez, G. I., & Sanabria-González, N. R. (2020). Adsorption of Cr(VI) in aqueous solution using a surfactant-modified bentonite. *The Scientific World Journal*, *2020*, 3628163. https://doi.org/10.1155/2020/3628163

[74] Gan, C., Liu, Y., Tan, X., Wang, S., Zeng, G., Zheng, B., Li, T., Jiang, Z., & Liu, W. (2015). Effect of porous zinc–biochar nanocomposites on Cr(VI) adsorption from aqueous solution. *RSC Advances*, *5*, 35107-35115. https://doi.org/10.1039/C5RA04416B

[75] Zimmermann, A. C., Mecabô, A., Fagundes, T., & Rodrigues, C. A. (2010). Adsorption of Cr(VI) using Fe-crosslinked chitosan complex (Ch-Fe). *Journal of Hazardous Materials*, *179*, 192-196. https://doi.org/10.1016/j.jhazmat.2010.02.078

[76] Rajapaksha, A. U., Selvasembian, R., Ashiq, A., Gunarathne, V., Ekanayake, A., Perera, V., Wijesekera, H., Mia, S., Ahmad, M., & Vithanage, M. (2022). A systematic review on adsorptive removal of hexavalent chromium from aqueous solutions: Recent advances. *Science of the Total Environment*, *809*, 152055. https://doi.org/10.1016/j.scitotenv.2021.152055

[77] Elangovan, R., Philip, L., & Chandraraj, K. (2008). Biosorption of chromium species by aquatic weeds: Kinetics and mechanism studies. *Journal of Hazardous Materials*, *152*, 100-112. https://doi.org/10.1016/j.jhazmat.2007.06.067

[78] Miretzky, P., & Cirelli, A. F. (2010). Cr(VI) and Cr(III) removal from aqueous solution by raw and modified lignocellulosic materials: A review. *Journal of Hazardous Materials*, *180*, 1-19. https://doi.org/10.1016/j.jhazmat.2010.04.060

How to cite this paper:

Dat, N. D., Huynh, S. Q., Nguyen, L. M. & Tran, H. N. (2026). Adsorption of hexavalent chromium from aqueous solution using glucose-derived spherical activated carbon: The role of functional groups. Advances in Environmental Technology, 12(3), 308-327. DOI: 10.22104/aet.2026.7860.2207